Asian Journal of Applied Sciences (ISSN: 2321 – 0893)
Volume 04 – Issue 02, April 2016

Numerical Analysis on Flow and Heat Transfer Behaviors in A Heating Tube with Various Attack Angles of Punched Delta Winglet Turbulators

Amnart Boonloi

Department of Mechanical Engineering Technology, College of Industrial Technology,
King Mongkut's University of Technology North Bangkok, Bangkok 10800, Thailand.
Email: amnartb [AT] kmutnb.ac.th

ABSTRACT— ***Numerical investigations on heat transfer and flow profiles in a circular tube at various parameters of punched delta winglet turbulators (PDWT) are reported. The effects of the flow blockage ratios, BR = 0.10 – 0.30, Reynolds numbers, Re = 100 – 2000, flow attack angles, α = 0^o, 15^o, 30^o and 45^o are investigated on both downstream and upstream arrangements. As the results, the presence of the PDWT in the tube heat exchanger can augment the heat transfer coefficient and thermo-hydraulic performance greater than the smooth tube with no turbulators. The swirling flow, vortex flow, impinging flow and turbulent mixing are phenomenas when installing with the PDWT in the tube that promotes to increase thermal efficiency. The optimum TEF is found when using the PDWT with BR = 0.30, Re = 2000, α = 30^o for upstream case. In addition, the use of the PDWT with the low flow blockage area can help to decrease the friction loss of the heating section.***

Keywords— circular tube, delta winglet, attack angle, flow visualization, heat transfer

1. INTRODUCTION

The turbulators are widely applied to develop the heating process of heat exchnagers. The swirling flow, vortex flow, impinging flow, which are created from the turbulators, can augment turbulent mixing in the heat exchangers that helps to improve overall efficiency of the heating section. Due to the effectiveness of the turbulators, many investigators had been studied the use of various turbulators in the heating system.

The winglet is a type of the turbulators, which always placed in fin-and-tube heat exchangers to augment the heat transfer rate. The winglet can generate longitudinal vortex flow and increase turbulent mixing of the test fluid. The numerical and experimental investigations, which focus on heat transfer augmentation by using various types of winglets, had been presented [1-12]. The researchers reported that the winglet turbulators give higher thermal performance than the smooth channel/tube heat exchanger.

As above, the conclusions are reported as follows;

- The use of the winglet turbulatos can increase the thermo-hydraulic performance by changing the flow structure and creating the vortex flow. The high flow blockage area of the winglet may lead to very large pressure in the heating or cooling systems.
- The use of the numerical investigations can report the results in terms of flow and heat transfer profiles. The understanding of these phenomenas is a key to develop compact heat exchangers.
- The flow attack angle, flow direction, winglet height, etc., are important factors that relate with the heat transfer characteristic and flow structure in the heat exchanger.
- The winglet, which formed by punching method, is convenient for production. The insertion in the middle of the circular tube heat exchange is easy to maintenance when installing in real systems.
- The delta shape of the winglet can help to decrease the friction loss in the heating section when comparing with rectangular shape.
- The delta winglet had been used to improve thermal performance in rectangular channel, square duct, fin-and-tube heat exchanger, etc. The use of the punched delta winglet pair in the heating circular tube has rarely been reported.

The aim of the current investigation is to study the flow topology and heat transfer profile in the circular tube heat exchanger with turbulators. The punched delta winglet turbulators (*PDWT*) are installed in the heating system to improve heat transfer coefficient. The influences of the flow attack angles, flow directions, blockage ratios and the Reynolds number of the *PDWT* in the tube heat exchanger are investigated numerically.

2. THE CIRCULAR TUBE CONFIGURATION, BOUNDARY CONDITION AND ASSUMPTION

2.1 Computational model

Figure 1 presents the *PDWT*s insert in the circular tube heat exchanger. The delta winglet are punched out from the smooth plate and inserted in the middle of the test tube. The tube diameter, *D*, is set to 0.05 m. The flow blockage ratio is computed from the ratio between winglet height, *b*, and tube diameter, *D*, (*b*/*D* is known as *BR*). The pitch ratio of the *PDWT* is calculated from the ratio between the winglet spacing and tube diameter, *PR* = 1. The case investigates are shown in Table 1.

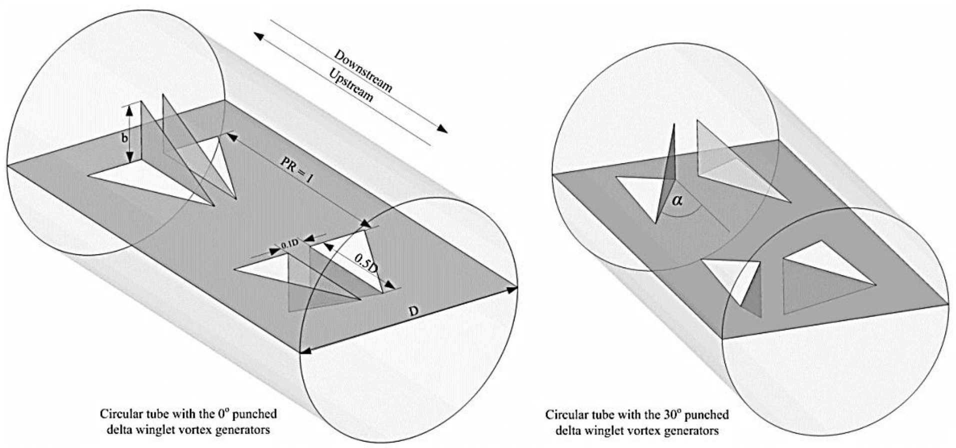

Figure 1 : Parameters of the *PDWT* in the circular tube heat exchanger.

Table 1 : Case studies of the *PDWT* in the circular tube heat exchanger.

Parameter	
Flow attack angle, α	0°, 15°, 30°, 45°
Reynolds number, *Re*	100 – 2000
Blockage ratio, *BR*	0.10, 0.15, 0.20, 0.25, 0.30
Flow directions	Winglet tip pointing downstream called “Downstream”, *WD* Winglet tip pointing upstream called “Upstream”, *WU*

2.2 Boundary conditions and numerical assumptions

The boundary conditions of the present study are reported as Table 2.

Table 2 : The boundary conditions for the *PDWT*.

Zone of the domain	**Boundary condition**
Inlet, outlet	Periodic boundary
Tube wall	Constant temperature with 310 K
Tested fluid	- Air at 300 K - Constant properties at the average temperature - Flows into the test tube with constant mass flow rate
PDWT and smooth plate	Adiabatic wall condition (insulator)

The numerical assumptions of the tube heat exchanger with *PDWT* are summarized as follows;

- Steady three–dimensional fluid flow and heat transfer.
- The flow is laminar and incompressible.
- The fluid properties are set at constant value.
- Body forces, viscous dissipation and radiation heat transfer are disregarded.

3. MATHEMATICAL FOUNDATIONS AND NUMERICAL METHOD

The mathematical foundation and numerical method of the present investigation are referred form *Ref.* [14]. The important parameters can be expressed as follows;

$$Re = \rho \bar{u} D / \mu \tag{1}$$

$$f = \frac{(\Delta p / L) D}{\frac{1}{2} \rho \bar{u}^2} \tag{2}$$

$$Nu_x = \frac{h_x D}{k} \tag{3}$$

$$TEF = \left.\frac{h}{h_0}\right|_{pp} = \left.\frac{Nu}{Nu_0}\right|_{pp} = \left(Nu/Nu_0\right)/\left(f/f_0\right)^{1/3} \tag{4}$$

4. NUMERICAL RESULT AND DISCUSSION

4.1 Validation with the smooth circular tube and grid independence

Figure 2 reports the verifications of the smooth tube for the heat transfer rate and pressure loss in terms of the Nusselt number and friction factor, respectively. It is found that the values from the current investigation and the values of the correlation [13] are in agreement; the deviation is found around ±0.03% on both the Nussslt number and friction factor. The grid independent test is done by comparing the number of grid cells on flow and heat transfer. The 120000, 240000, 360000 and 480000 cells of the grid are set for the current computational domain at *BR* = 0.30, *Re* = 2000, $\alpha = 45^o$, of the *WD-PDWT*. As the results, the Nusselt number and friction factor values are very close when increasing grid cells from 240000 to 360000, hence, it is not advantage to increase grid cells to 360000. The 240000 cells are selected for the current computational domain.

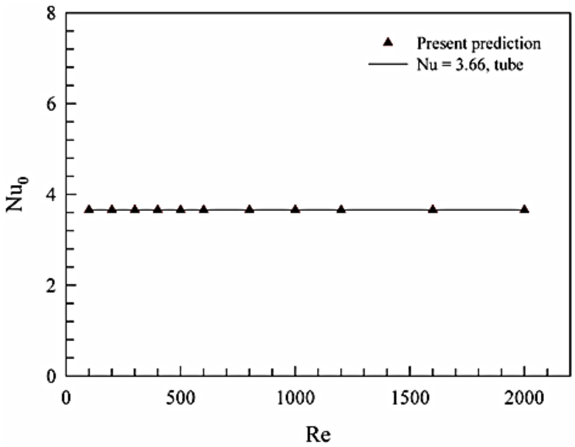

(a)

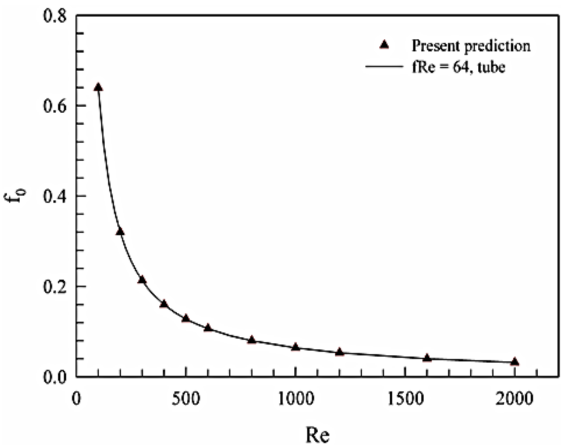

(b)

Figure 2 : Verifications of the smooth result for (a) *Nu* and (b) *f*.

4.2 Flow and heat transfer behaviors

Figure 3 presents the flow patterns in y-z planes for the *PDWT* with the flow attack angles of 0^o, 15^o, 30^o and 45^o at *Re* = 2000 and *BR* = 0.30. As the figure, it is found that the *PDWT* with the flow attack angles of 15^o, 30^o and 45^o can promote the vortex flows or swirling flows through the test section. The four main vortex flows and small vortices near the tube wall are produced by *PDWT*. Considering at the lower pair of the vortex stream, the *WD-PDWT* performs the counter rotating flow with common-flow-up, while the *WU-PDWT* produces similar flow pattern with common-flow-down. The generation of the vortex flow and small vortices is due to the pressure difference between in front of the *PDWT* and behind the *PDWT*. The *PDWT* with the flow attack angle of 0^o cannot create the vortex flow in the test section. The higher of the flow attack angle leads to the higher of the vortex strength or vortex intensity. The flow attack angle of 45^o provides the highest vortex strength, while the flow attack angle of 0^o performs the reversed result.

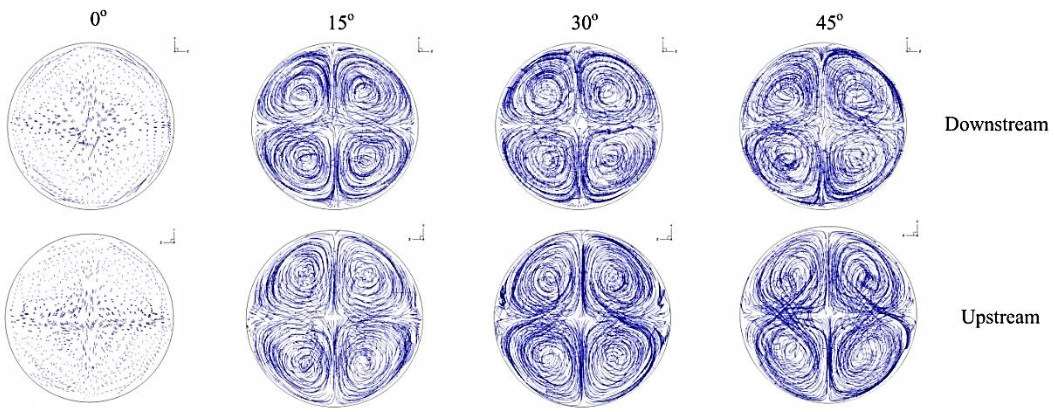

Figure 3 : flow patterns in y-z plane of the *PDWT* at *BR* = 0.30 and *Re* = 1200.

Figures 4*a*, *b*, *c* and *d* show the temperature patterns in y-z planes for the *WD-PDWT* at *Re* = 2000, *BR* = 0.30 for the flow attack angles of 0^o, 15^o, 30^o and 45^o, respectively. As the numerical result, it is found that the flow attack angle of 0^o obviously presents the highest thickness of the red contour at near the tube wall. The thickness of the red layer decreases when increasing the flow attack angle. The flow attack angle of 45^o provides the lowest red layer of the contour temperature near the tube wall. The reduction of the red layer is due to the better mixing of the fluid flow, especially, at high vortex strength. The similar patterns are reported in the Figure 5*a*, *b*, *c*, *d* and *e* for the *WU-PDWT* with the flow attack angles of 0^o, 15^o, 30^o and 45^o, respectively, for *Re* = 2000 and *BR* = 0.30. Figures 6*a*, *b*, *c*, *d* and *e* display the temperature patterns in y-z planes for the *WD-PDWT* at *BR* = 0.10, 0.15, 0.20, 0.25 and 0.30, respectively, at *Re* = 1000 and $\alpha = 30^o$. The *BR* = 0.3 provides the best mixing, while the *BR* = 0.10 is the worst case.

The local Nusselt number on the tube wall are reported in the Figures 7*a*, *b*, *c*, *d* and *e* for the flow attack angles of 0^o, 15^o, 30^o and 45^o, respectively, at *Re* = 2000, *BR* = 0.3 and *WD-PDWT*. In general, the use of the *PDWT* in the tube heat exchanger leads to higher heat transfer rate than the smooth circular tube with no vortex generators. The flow attack angle of 45^o gives the highest heat transfer rate due to the highest vortex strength and the best fluid mixing. The flow attack angle of 30^o provides higher heat transfer rate than the flow attack angle of 15^o, while the flow attack angle of 0^o gives the lowest value of heat transfer rate. The similar trends of the heat transfer are found when using the *WU-PDWT* as depicted in the Figure 8*a*, *b*, *c* and *d* for the flow attack angles of 0^o, 15^o, 30^o and 45^o, respectively, at *Re* = 2000 and *BR* = 0.30. However, the difference of the flow structure leads to the difference of the heat transfer characteristics. The peaks of the heat transfer regimes are found at left and right parts of the tube when using the *WD-PDWT*, while the *WU-PDWT* produces the peak region of the heat transfer rate at the upper and lower parts of the tube (see Figure 9).

Figures 10*a*, *b*, *c*, *d* and *e* report the local Nusselt number distributions on the circular tube wall for the *WD-PDWT* with the *BR* = 0.10, 0.15, 0.20, 0.25 and 0.30, respectively, at *Re* = 1000 and $\alpha = 30^o$. The peak of heat transfer regime is found similar for all *BR* values. The *BR* = 0.3 performs the highest heat transfer rate, while the *BR* = 0.10 gives the lowest value. In conclusion, the strength of the vortex flow, impinging flow and turbulent mixing increases when rising *BR*.

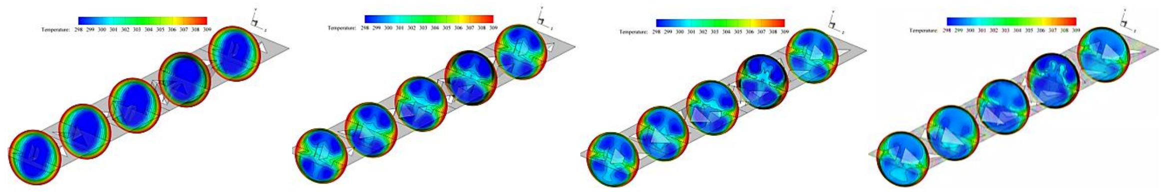

(a) (b) (c) (d)

Figure 4 : Temperature patterns in y-z plane of the *WD-PDWT* for the flow attack angle of (a) 0^o, (b) 15^o, (c) 30^o and (d) 45^o at *BR* = 0.30, *Re* = 1200.

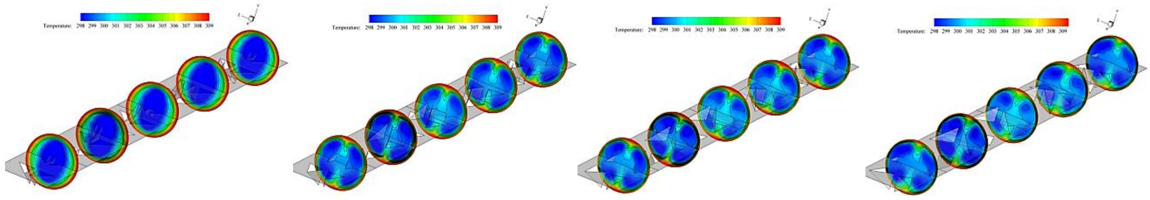

(a) (b) (c) (d)

Figure 5 : Temperature patterns in y-z plane of the *WU-PDWT* for the flow attack angle of (a) 0^o, (b) 15^o, (c) 30^o and (d) 45^o at *BR* = 0.30, *Re* = 1200.

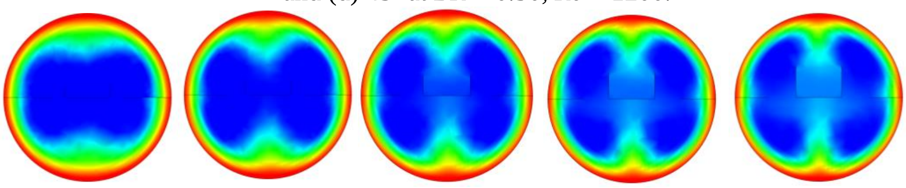

(a) (b) (c) (d) (e)

Figure 6 : Temperature patterns in y-z plane of the *WD-PDWT* for (a) *BR* = 0.10, (b) *BR* = 0.15, (c) *BR* = 0.20, (d) *BR* = 0.25 and (e) *BR* = 0.30 at $\alpha = 30^o$, *Re* = 1200.

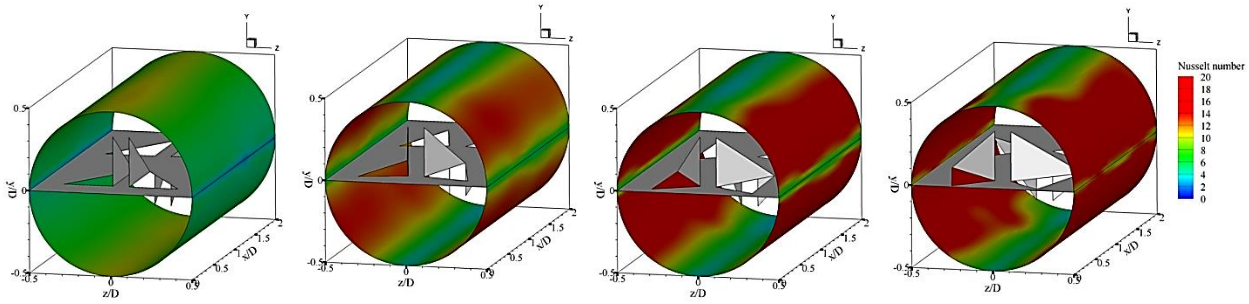

(a) (b) (c) (d)

Figure 7 : Local Nusselt number patterns on the tube wall of the *WD-PDWT* for the flow attack angle of (a) 0^o, (b) 15^o, (c) 30^o and (d) 45^o at *BR* = 0.30, *Re* = 1200.

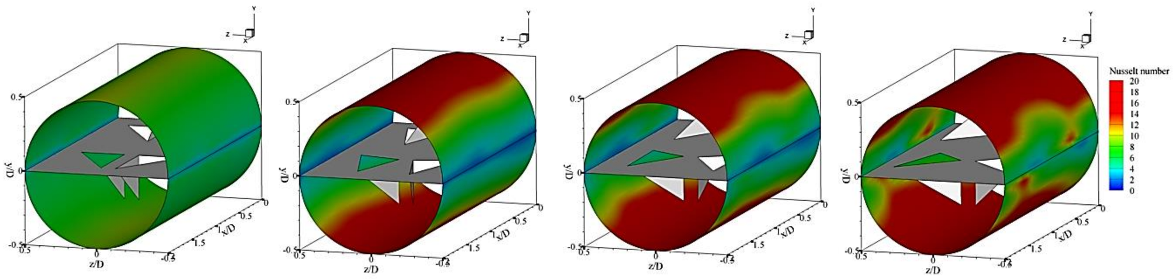

(a) (b) (c) (d)

Figure 8: Local Nusselt number patterns on the tube wall of the *WU-PDWT* for the flow attack angle of (a) 0^o, (b) 15^o, (c) 30^o and (d) 45^o at *BR* = 0.30, *Re* = 1200.

4.3 Thermal performance evaluation

4.3.1 Heat transfer

The variations of the Nu/Nu_0 with the Reynolds number at various *BR* and flow direction for the flow attack angles of 0^o, 15^o, 30^o and 45^o are presented in the Figures 11*a*, *b*, *c* and *d*, respectively. In general, the rise of the Reynolds number and *BR* leads to increase in the Nu/Nu_0 for all cases.

At $\alpha = 0^o$, the *WD-PDWT* performs slightly higher Nu/Nu_0 than the *WU-PDWT* when the *BR* > 0.10. The use of the *WD-PDWT* with the flow attack angle of 0^o gives the heat transfer rate around 1.95, 1.96, 1.98, 2.01 and 2.06 times higher than the smooth tube with no turbulators for *BR* = 0.10, 0.15, 0.20, 0.25 and 0.30, respectively, and around 1.94, 1.95, 1.97, 2.00 and 2.04 times for the *WU-PDWT* at *Re* = 2000.

At $\alpha = 15^o$, the *WU-PDWT* provides higher heat transfer rate than the *WD-PDWT* for all the flow blockage ratios and Reynolds number values. The maximum Nu/Nu_0 is around 2.22, 2.67, 3.02, 3.25 and 3.44 for the *WD-PDWT* and around 2.29, 2.78, 3.30, 3.75 and 4.14 for the *WU-PDWT* at *BR* = 0.10, 0.15, 0.20, 0.25 and 0.30, respectively. It is noted that the variance of the Nu/Nu_0 between the *WU-PDWT* and *WD-PDWT* is found to be larger when the *BR* higher than 0.15.

The variations of the Nu/Nu_0 with the Reynolds number for the flow attack angle of 0^o are found similar as the flow attack angle of 15^o. The *WU-PDWT* with *BR* = 0.30, *Re* = 2000 performs the highest heat transfer rate around 5.14 times higher than the smooth tube with no vortex generators. In range studies, the *PDWT* gives the Nusselt number around 1.30 – 5.14 times higher than the smooth tube for the flow attack angle of 30^o.

The *WU-PDWT* with the flow attack angle of 45^o, which gives the best vortex strength and fluid mixing, shows the optimum heat transfer rate around 5.7 times higher than the smooth tube for *BR* = 0.30, *Re* = 2000. The *WU-PDWT* provides higher heat transfer rate than the *WD-PDWT* for all *BR* and *Re* values. In range investigates, the *PDWT* can enhance heat transfer rate around 1.30 – 5.70 times higher than the smooth case when using 45^o *PDWT*.

The flow attack angle of 45^o of the *PDWT* performs the highest Nu/Nu_0 due to the highest vortex strength/vortex intensity and the best fluid mixing in the test section. The *PDWT* with the flow attack angle of 30^o provide higher Nu/Nu_0 than the flow attack angle of 15^o when considered at similar conditions. The lowest Nu/Nu_0 is detected for the *PDWT* with the flow attack angle of 0^o due to the weakest vortex flow. The use of the *PDWT* not only increases in heat transfer rate, but also increases in the friction loss.

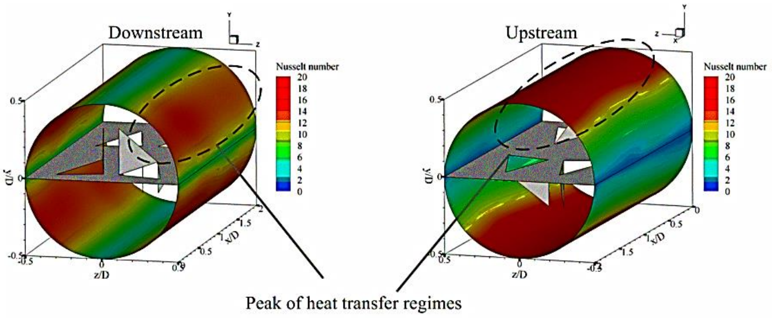

Figure 9 : The peak of heat transfer regime on the tube surfaces.

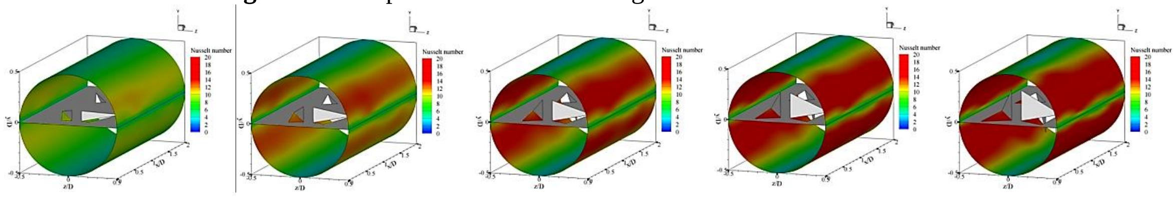

(a) (b) (c) (d) (e)

Figure 10 : Temperature patterns on the tube wall of the *WD-PDWT* for (a) *BR* = 0.10, (b) *BR* = 0.15, (c) *BR* = 0.20, (d) *BR* = 0.25 and (e) *BR* = 0.30 at $\alpha = 30^o$, *Re* = 1200.

4.3.2 Pressure loss

The pressure loss is presented in term of the variations of the f/f_0 with the Reynolds number with various flow directions, *BR*s, *Re* and flow attack angles as Figures 12*a*, *b*, *c* and *d*, respectively, for the flow attack angle of 0^o, 15^o, 30^o and 45^o of the *PDWT*. In general, the presence of the *PDWT* leads to higher friction factor than the smooth circular tube for all generators. The f/f_0 tends to increase with the rise of the Reynolds number for all cases. The decrease of the *BR* can reduce the pressure loss in the test section. The *BR* = 0.30 performs the highest friction factor, while the *BR* = 0.10 gives the lowest value.

At $\alpha = 0^o$, the f/f_0 for both cases shows nearly values for all *BR* and *Re* values. The use of the *PDWT* in the tube heat exchanger with the flow attack angle of 0^o provides the friction factor around 3 – 6.25 times higher than the smooth circular tube.

At $\alpha = 15^o$, the *WD-PDWT* gives slightly higher friction factor than the *WU-PDWT* for all *BR*s. The f/f_0 is around 3 – 8.3 when using the 15^o *PDWT*.

At $\alpha = 30^o$, the similar results as the flow attack angle of 15^o are found in the *BR* = 0.10 – 0.25. The both cases provide nearly value of the f/f_0 at *BR* = 0.3. In range studies, the friction factor of the *PDWT* is around 3 – 13 times higher than the base case.

At $\alpha = 45^o$, the f/f_0 of the *PDWT* at *BR* = 0.10 is found to be equal for both cases. When *BR* > 0.10, the *WU-PDWT* performs higher f/f_0 than the *WD-PDWT*. In range investigates, the use of the 45^o *PDWT* gives f/f_0 around 3 – 20.

For $\alpha = 0^o$, 15^o and 20^o, the *WD-PDWT* gives slightly higher friction loss than the *WU-PDWT*. The rise of the flow attack angle leads to increasing friction loss. The flow attack angle of 45^o provides the highest friction loss, while the flow attack angle of 30^o performs higher friction factor than the flow attack angle of 15^o. The flow attack angle of 0^o gives the lowest friction loss due to the low flow blockage area when considered at cross sectional area.

4.3.3 Thermal enhancement factor

The performance of the circular tube heat exchanger with the *PDWT* in term of thermal enhancement factor (*TEF*) is computed from the Nu/Nu_0 and f/f_0. Figure 13*a*, *b*, *c* and *d* present the variations of the *TEF* with the Reynolds number with various cases. Generally, the *TEF* increases with increasing the Reynolds number for all cases. The flow attack angle of 0^o on both cases provides the lowest *TEF*. The *WD-PDWT* at *BR* = 0.30, *Re* = 2000 gives the maximum *TEF* around 1.70, 1.80 and 1.87 for the flow attack angles of 15^o, 30^o and 45^o. respectively. The *WU-PDWT* at *BR* = 0.30 shows the optimum *TEF* around 2.05, 2.18 and 2.08, respectively, for the flow attack angles of 15^o, 30^o and 45^o at the highest Reynolds number.

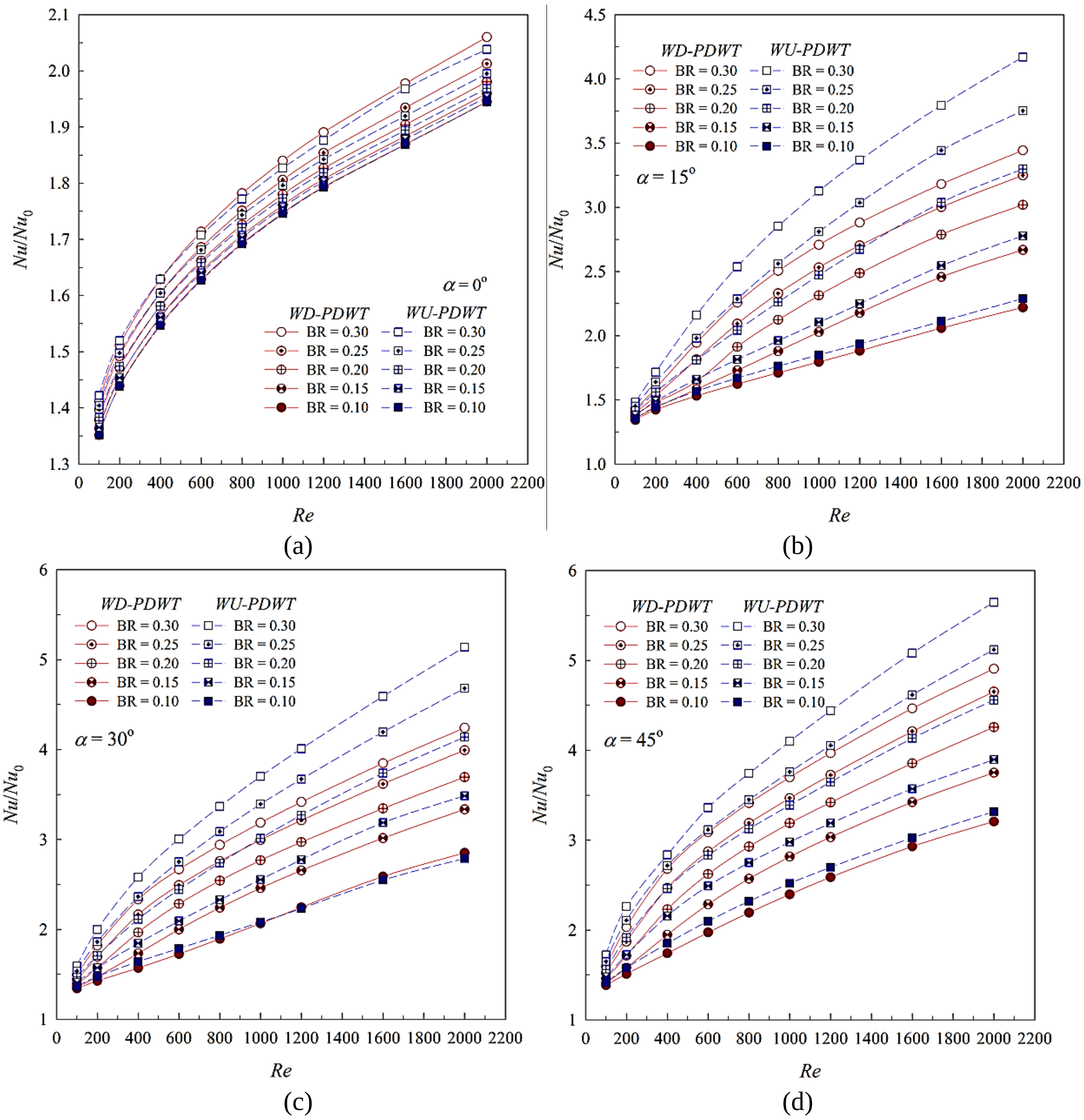

Figure 11 : Nu/Nu_0 versus *Re* of the *WD-PDWT* and *WU-PDWT* for the flow attack angle (a) 0°, (b) 15°, (c) 30° and (d) 45°.

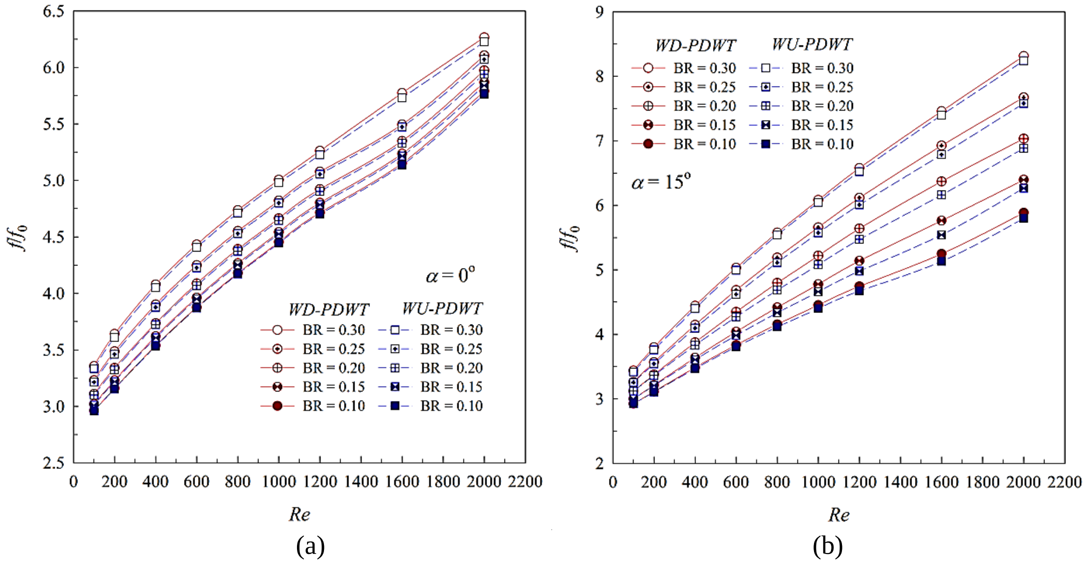

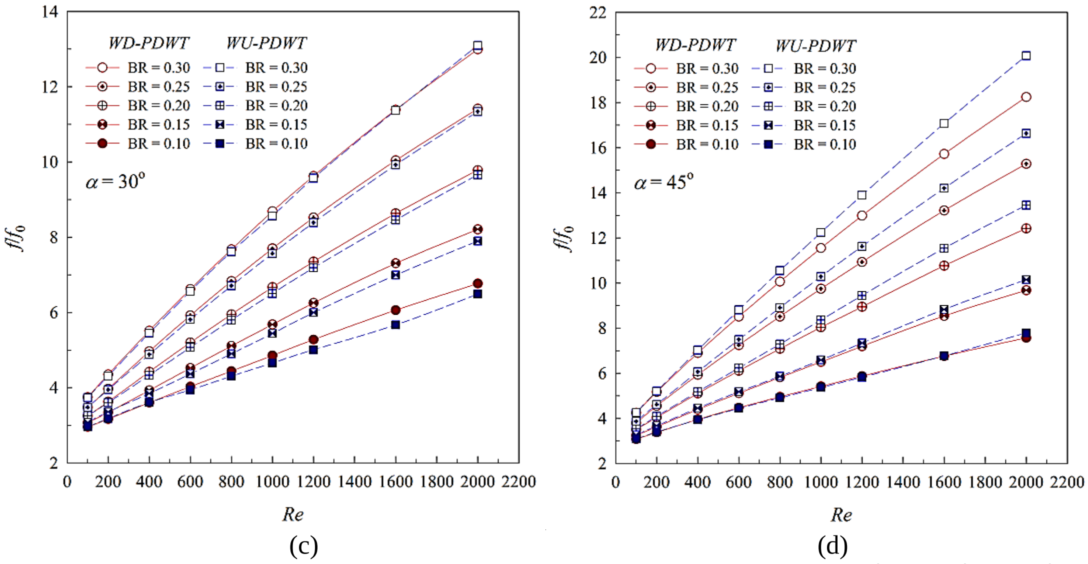

Figure 12 : f/f_0 versus *Re* of the *WD-PDWT* and *WU-PDWT* for the flow attack angle (a) 0°, (b) 15°, (c) 30° and (d) 45°.

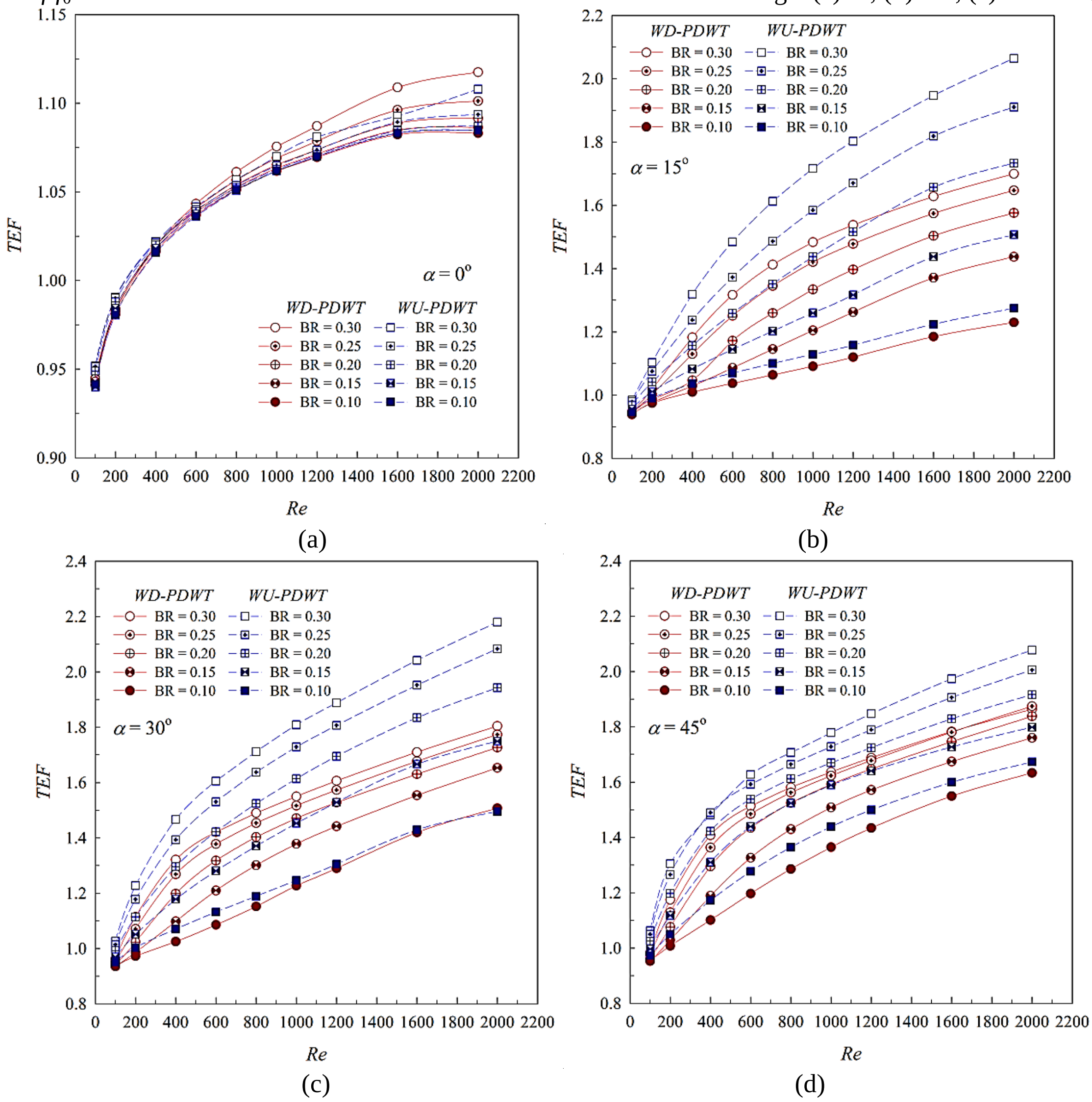

Figure 13 : *TEF* versus *Re* of the *WD-PDWT* and *WU-PDWT* for the flow attack angle (a) 0°, (b) 15°, (c) 30° and (d) 45°.

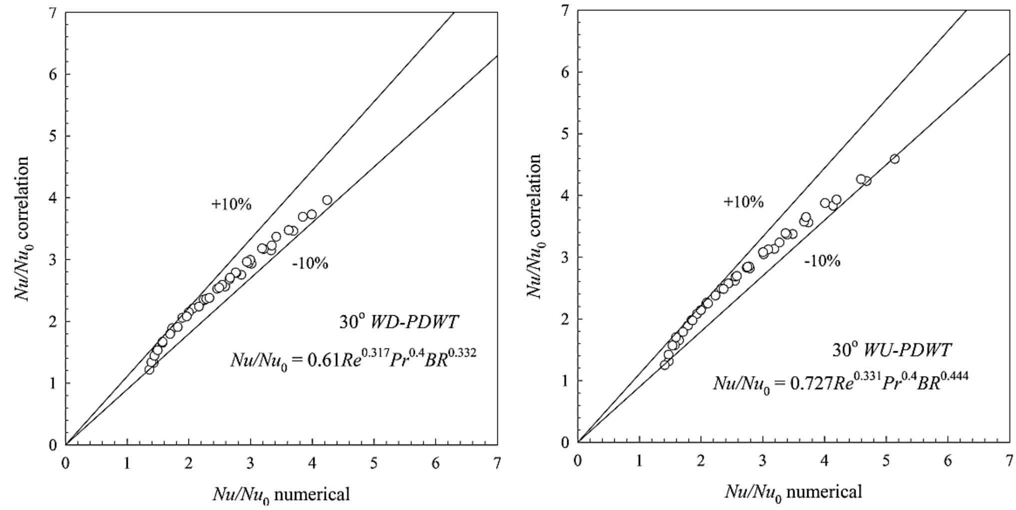

(a) (b)

Figure 14 : Correlations of the Nu/Nu_0 for the 30^o of (a) *WD-PDWT* and (b) *WU-PDWT*.

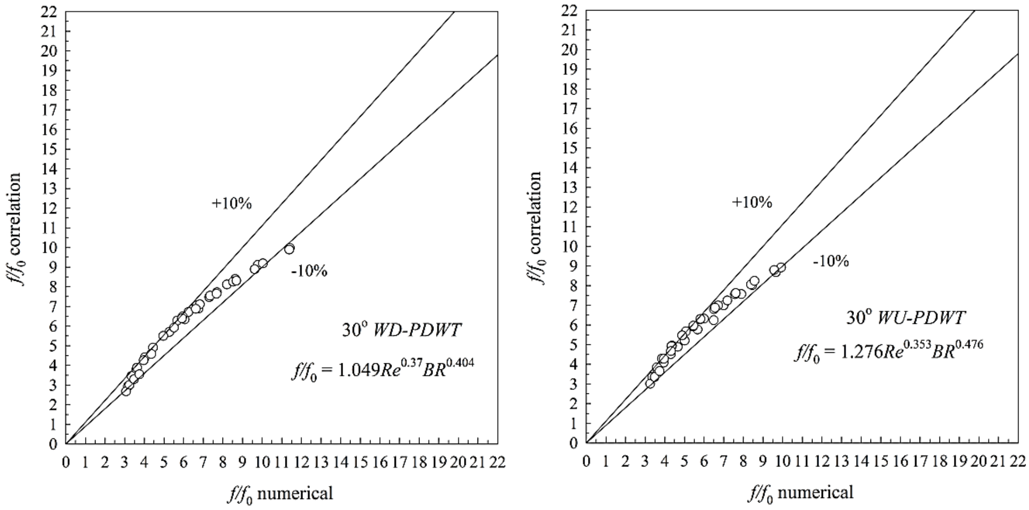

(a) (b)

Figure 15 : Correlations of the f/f_0 for the 30^o of (a) *WD-PDWT* and (b) *WU-PDWT*.

5. CONCLUSION

The numerical investigations on heat transfer, flow visualization and thermal performance evaluation in the circular tube heat exchanger with various parameters of the *PDWT* are presented. The main findings are concluded as follows:

- The use of the *PDWT* can enhance the heat transfer rate and thermal performance due to the creation of the vortex flow, swirling flow and impinging flow.
- In range investigates, the augmentations of the heat transfer rate and friction loss are detected to be maximum around 5.7 and 20 times higher than the smooth circular tube with no generators, respectively. The optimum *TEF* around 2.18 is ibtained at BR = 0.30, Re = 2000, α = 30^o for *WU-PDWT*.
- The correlations of the Nu/Nu_0 for the 30^o *WD-PDWT* and *WU-PDWT* are reported in the Figures 16*a* and *b*, respectively, while the Figures 17*a* and *b* present the correlations of the f/f_0 for *WD-PDWT* and *WU-PDWT*, respectively. The equations (5) – (8) present the empirical correlations of the 30^o *PDWT* in the heating tube.

$$Nu / Nu_0 = 0.61\,\mathrm{Re}^{0.317}\,\mathrm{Pr}^{0.4}\,BR^{0.332}\text{ , }\textit{WD-PDWT} \quad (5)$$

$$Nu / Nu_0 = 0.727\,\mathrm{Re}^{0.331}\,\mathrm{Pr}^{0.4}\,BR^{0.444}\text{ , }\textit{WU-PDWT} \quad (6)$$

$$\mathrm{f}/\,\mathrm{f}_0 = 1.049\,\mathrm{Re}^{0.37}\,BR^{0.404}\text{ , }\textit{WD-PDWT} \quad (7)$$

$$\mathrm{f}/\,\mathrm{f}_0 = 1.276\,\mathrm{Re}^{0.353}\,BR^{0.476}\text{ , }\textit{WU-PDWT} \quad (8)$$

NOMENCLATURE

D	diameter of a circular tube
f	friction factor
h	convective heat transfer coefficient, W m^{-2} K^{-1}

k	thermal conductivity, W m^{-1} K^{-1}
Nu	Nusselt number
p	static pressure, Pa
Pr	Prandtl number
Re	Reynolds number,
T	temperature, K
u_i	velocity in xi-direction, m s^{-1}
Greek letter	
μ	dynamic viscosity, kg $s^{-1}m^{-1}$
Γ	thermal diffusivity
α	flow attack angle, degree
TEF	thermal enhancement factor, $(=(Nu/Nu_0)/(f/f_0)^{1/3})$
ρ	density, kg m^{-3}
Subscript	
in	inlet
0	smooth circular tube
pp	pumping power

6. ACKNOWLEDGEMENT

This researcher was funded by College of Industrial Technology, King Mongkut's University of Technology North Bangkok, Thailand. The researchers would like to thank Dr. Withada Jedsadaratanachai and Assoc. Prof. Dr. Pongjet Promvonge for suggestions.

7. REFERENCES

[1] P. Promvonge, S. Suwannapan, M. Pimsarn and C. Thianpong, "Experimental study on heat transfer in square duct with combined twisted-tape and winglet vortex generators", International Communications in Heat and Mass Transfer, Elsevier, vol. 59, pp. 158-165, 2014.

[2] S. Chokphoemphun, M. Pimsarn, C. Thianpong and P. Promvonge, "Heat transfer augmentation in a circular tube with winglet vortex generators", Chinese Journal of Chemical Engineering, Elsevier, vol. 23(4), pp. 605-614, 2015.

[3] S. Caliskan, "Experimental investigation of heat transfer in a channel with new winglet-type vortex generators", International Journal of Heat and Mass Transfer, Elsevier, vol. 78, pp. 604-614, 2014.

[4] A.A. Gholami, M.A. Wahid and H.A. Mohammed, "Heat transfer enhancement and pressure drop for fin-and-tube compact heat exchangers with wavy rectangular winglet-type vortex generators", International Communications in Heat and Mass Transfer, Elsevier, vol. 54, pp. 132-140, 2014.

[5] G. Zhou and Z. Feng, "Experimental investigations of heat transfer enhancement by plane and curved winglet type vortex generators with punched holes", International Journal of Thermal Sciences, Elsevier, vol. 78, pp. 26-35, 2014.

[6] P. Saha, G. Biswas and G. Sarkar, "Comparison of winglet-type vortex generators periodically deployed in a plate-fin heat exchanger – A synergy based analysis", International Journal of Heat and Mass Transfer, Elsevier, vol. 74, pp. 292-305, 2014.

[7] M. Khoshvaght-Aliabadi, O. Sartipzadeh and A. Alizadeh, "An experimental study on vortex-generator insert with different arrangements of delta-winglets", Energy, Elsevier, vol. 82, pp. 629-639, 2015.

[8] A. Abdollahi and M. Shams, "Optimization of shape and angle of attack of winglet vortex generator in a rectangular channel for heat transfer enhancement", Applied Thermal Engineering, Elsevier, vol. 81, pp. 376-387, 2015.

[9] Y.L. He, P. Chu, W.Q. Tao, Y.W. Zhang and T.Xie, "Analysis of heat transfer and pressure drop for fin-and-tube heat exchangers with rectangular winglet-type vortex generators", Applied Thermal Engineering, Elsevier, vol. 61(2), pp. 770-783, 2013.

[10] H.Y. Li, C.L. Chen, S.M. Chao and G.F. Liang, "Enhancing heat transfer in a plate-fin heat sink using delta winglet vortex generators", International Journal of Heat and Mass Transfer, Elsevier, vol. 67, pp. 666-677, 2013.

[11] H. Huisseune, C. T'Joen, P.D. Jaeger, B. Ameel, S.D. Schampheleire and M.D. Paepe, "Performance enhancement of a louvered fin heat exchanger by using delta winglet vortex generators", International Journal of Heat and Mass Transfer, Elsevier, vol. 56(1-2), pp. 475-487, 2013.

[12] A. Colleoni, A. Toutant, G. Olalde and J.M. Foucaut, "Optimization of winglet vortex generators combined with riblets for wall/fluid heat exchange enhancement", Applied Thermal Engineering, Elsevier, vol. 50(1), pp. 1092-1100, 2013.

[13] F. Incropera and P.D. Dewitt, " Introduction to Heat Transfer, 5th ed.", John Wiley & Sons, 2006.

[14] P. Promvonge, W. Jedsadaratanachai and S. Kwankaomeng, "Numerical study of laminar flow and heat transfer in square channel with 30° inline angled baffle turbulators", Applied Thermal Engineering, vol. 30 (11-12), pp. 1292-1303, 2010.